

Simplified Synthetic Approach to Tetrabrominated Spiro-Cyclopentadithiophene and the Following Derivation to A-D-A Type Acceptor Molecules for Use in Polymer Solar Cells

Xiaochen Liu, Yuanxun Zhang, Jianchang Wu, Yuchao Ma, Kim K. T. Lau, Jin Fang, Chang-Qi Ma, and Yi Lin*



Cite This: *J. Org. Chem.* 2022, 87, 5057–5064



Read Online

ACCESS |



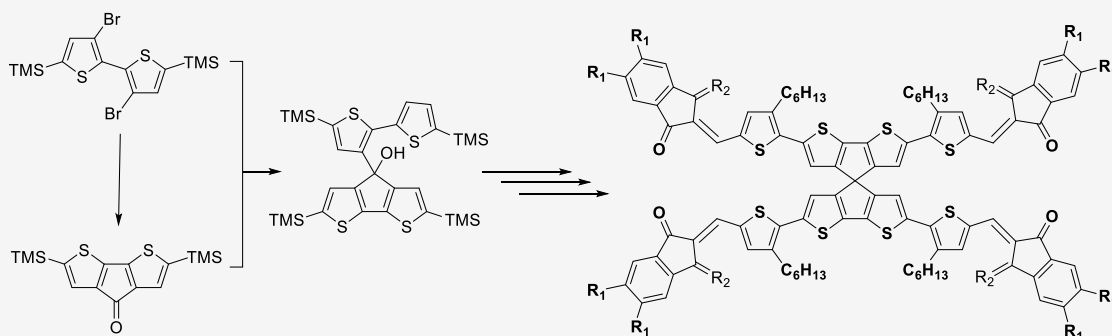
Metrics & More



Article Recommendations



Supporting Information



ABSTRACT: 4,4'-Spiro-bis[cyclopenta[2,1-*b*:3,4-*b'*]dithiophene] (SCT) is a versatile building block for constructing three-dimensional (3D) π -conjugated molecules for use in organic electronics. In this paper, we report a more convenient synthetic route to SCT and its derivatives, where a structurally symmetric 3,3'-dibromo-5,5'-bis(trimethylsilyl)-2,2'-bithiophene (**2**) serves as the precursor for both the synthesis of 4*H*-cyclopenta[2,1-*b*:3,4-*b'*]dithiophen-4-one (**4**) and 4-(5,5'-bis(trimethylsilyl)-2,2'-bithiophen-3-yl)-2,6-bis(trimethylsilyl)-4-hydroxy-cyclopenta[2,1-*b*:3,4-*b'*]dithiophene (**5**). The later one is the key intermediate for the final brominated SCT building block. Such a “two birds with one stone” strategy simplifies the synthetic approach to the SCT core. Functionalization on the SCT core with different terminal electron-deficient groups, including 1*H*-indene-1,3(2*H*)-dione (**ID**), 2-(3-oxo-2,3-dihydro-1*H*-inden-1-ylidene)malononitrile (**IC**), and 2-(5,6-difluoro-3-oxo-2,3-dihydro-1*H*-inden-1-ylidene)malononitrile (**FIC**), was carried out, yielding three spiro-conjugated A-D-A type molecules, SCT-(**TID**)₄, SCT-(**TIC**)₄, SCT-(**TFIC**)₄, respectively. The optical spectroscopy and electrochemical properties of these three compounds were investigated and compared to the corresponding linear oligomers. Results revealed that the **IC** and **TFIC** terminated compounds showed low-lying HOMO/LUMO energy levels with reduced optical bandgap, making them more suitable for use in polymer solar cells. A power conversion efficiency of 3.73% was achieved for the SCT-(**TFIC**)₄ based cell, demonstrating the application perspective of 3D molecules.

INTRODUCTION

Organic semiconductors based on π -conjugated molecules have shown broad application prospects in organic electronics, including light emitting diodes (OLED),¹ organic field effect transistors (OFET),² organic photovoltaics (OPV),^{3,4} and perovskite solar cells (PSC).⁵ Up to now, conjugated molecules with different spatial dimensions have been developed, including 0-dimensional fullerene molecules,⁶ one-dimensional linear conjugated polymers⁷ and oligomers,⁸ graphene-like⁹ or cruciform-like two-dimensional molecules,¹⁰ as well as three-dimensional conjugated dendrimers¹¹ and spiro-compounds.¹² Owing to their unique orthogonal structure and the consequent intensive intermolecular interactions, 9,9'-spirobifluorene (SBF)-cored three-dimensional (3D) conjugated molecules are among the most intensively studied organic semiconductors, especially for OLEDs as the blue emitters,¹² for perovskite solar

cells as the hole transporting materials (HTM),⁵ and for polymer solar cells as the nonfullerene acceptor (NFA).^{13–15} As one example, Yang et al. recently reported the annulation of SBF with thiophene units to increase the π -conjugation length, which is able to increase the charge carrier mobility and a high PCE of 10.16% was achieved when blended with PBDB-T-2Cl.¹⁶

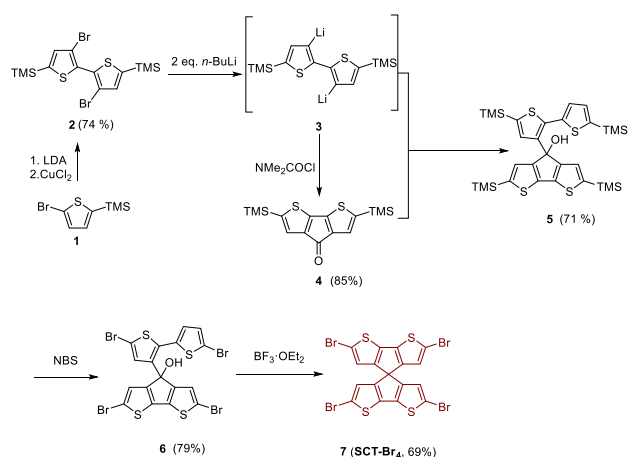
In comparison with the phenyl group, the thiophene unit showed characteristics such as lower resonance energy, ease of structure modification, higher charge carrier mobility, and it is a

Received: November 23, 2021

Published: March 25, 2022



Scheme 1. Synthetic Approach to 2,2',6,6'-Tetrabromo-4,4'-spiro[cyclopenta[2,1-*b*:3,4-*b'*]dithiophene] (SCT-Br₄) Starting from 2-Bromo-5-(trimethylsilyl)thiophene



fundamental building block for conjugated polymers and oligomers.¹⁷ Replacing the phenyl ring of SBF with thiophene yields a new spiro-conjugated core unit, 4,4'-spiro[cyclopenta[2,1-*b*;3,4-*b'*]dithiophene] (SCT, Scheme 1). Salbeck et al. first reported the electronic properties of SCT and its phenyl terminated compounds.¹⁸ Owing to the extended π -conjugation of the cyclopentadithiophene core, the SCT based compound showed smaller optical band gap and better field effect transistor effect than the SBF analogues. The SCT-cored molecules were also reported as dopant-free HTM for use in perovskite solar cells,¹⁹ and as NFA in polymer solar cells,^{20–22} demonstrating the SCT is a useful building block for the synthesis of conjugated 3D molecules for organic electronics.

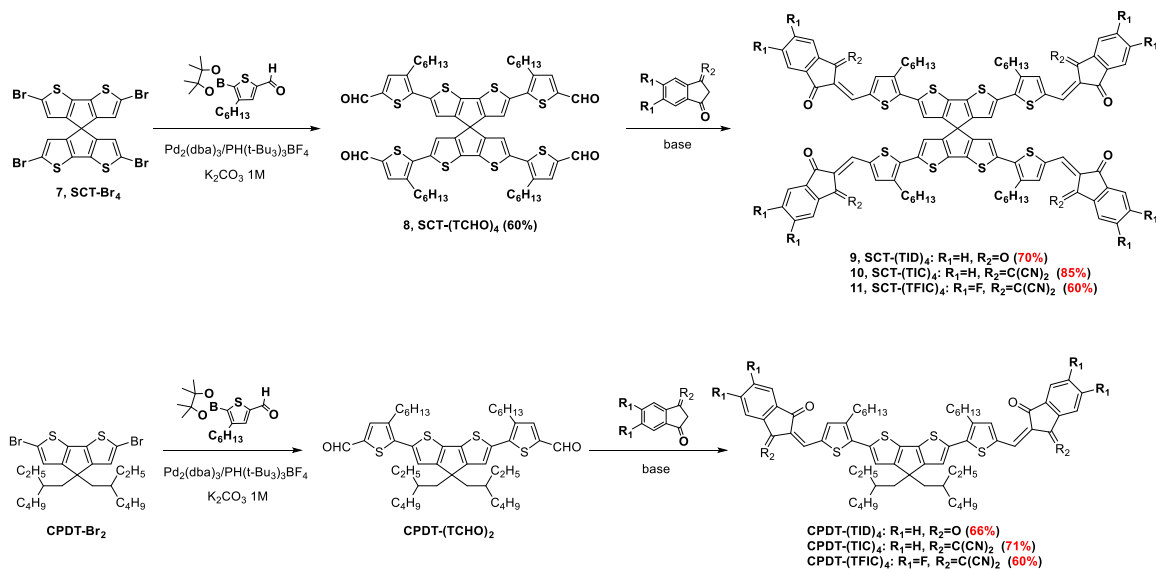
The synthesis approach to SCT was reported by Fungo et al. in 2013, where 3-bromo-2,2'-bithiophene was used as the key intermediate.²³ In this paper, we developed a more convenient synthetic strategy to the SCT core by using symmetric 3,3'-dibromo-5,5'-bis(trimethylsilyl)-2,2'-thiophene as the key intermediate. The use of symmetric intermediate significantly simplified the synthesis approach to SCT. Derivation of the SCT

core with different electron deficient terminal groups was demonstrated, and the use of these SCT-cored molecules in polymer solar cells were investigated. The current work enriches the molecular family of the SCT based spiro-conjugated molecules.

RESULTS AND DISCUSSIONS

Synthesis. The new synthesis approach to SCT is shown in Scheme 1, where structurally symmetric 3,3'-dibromo-5,5'-bis(trimethylsilyl)-2,2'-thiophene **2** was synthesized in a yield of 74% by a “halogen dancing” reaction of 2-bromo-3-(trimethylsilyl)thiophene **1** with LDA and the following CuCl₂ catalyzed homocoupling reaction.^{24–26} Lithiation of **2** with 2-fold *n*-BuLi yielded bis-lithiated intermediate **3** through the Li–Br exchange reaction, which can be converted to 2,6-bis(trimethylsilyl)-cyclopenta[2,1-*b*;3,4-*b'*]dithiophen-4-one **4** through a nucleophilic substitution reaction (yield of 85%). At the opposite to the reported procedure using a monobrominated bithiophene, this later can be advantageously substituted by compound **2**. After its bislithiation with 2 equiv of BuLi, it reacts with ketone **4** to yield 4-(5,5'-bis(trimethylsilyl)-2,2'-bithiophen-3-yl)-2,6-bis(trimethylsilyl)-4-hydroxy-cyclopenta[2,1-*b*;3,4-*b'*]dithiophene **5** (with a yield of 71%). Bromination of **5** with N-bromo-succinimide (NBS) in THF yields brominated compound **6** (79%), which was cyclized by a Friedel–Crafts cyclization at a mild condition using BF₃·OEt₂ as Lewis acid catalyst to yield the key building block 2,2',6,6'-tetrabromo-4,4'-spiro[cyclopenta[2,1-*b*;3,4-*b'*]dithiophene] **7** in a yield of 69%. It is worth pointing out that linear oligomer byproducts were also found for this reaction, which was ascribed to the intermolecular coupling reaction. Purification of compound **7** can be successfully achieved by size exclusion chromatography using Bio-Rad beads S-X1 as the stationary phase. Cyclization of **5** using the same cyclization condition was also performed. However, owing to the labile TMS groups under acidic conditions, complicated byproducts, including high molecular weight oligomers, also formed. Thus, substitution of TMS group by Br prior to the intramolecular cyclization is essential for successful synthesis of SCT-Br₄.

Scheme 2. Synthesis of SCT Cored A-D-A Derivatives and the Corresponding Linear Oligomers



Peripheral functionalization of the SCT-Br₄ was then completed in two steps (Scheme 2). First, Suzuki coupling reaction of SCT-Br₄ with 4-hexyl-5-(4,4,5,5-tetramethyl-1,3,2-dioxaborolan-2-yl)thiophene-2-carbaldehyde (B-TCHO) led to the aldehyde terminated new building block SCT-(TCHO)₄ in a yield of 60%. The following Knoevenagel condensation of SCT- with 1*H*-indene-1,3(2*H*)-dione (ID), 2-(3-oxo-2,3-dihydro-1*H*-inden-1-ylidene)malononitrile (IC), and 2-(5,6-difluoro-3-oxo-2,3-dihydro-1*H*-inden-1-ylidene)malononitrile (FIC), in the presence of base catalyst (piperidine or pyridine), gave the corresponding target spiro-conjugated molecules with an A-D-A substructure. It is worth pointing out that piperidine works better for coupling SCT-(TCHO)₄ with ID, while pyridine is the preferred catalyst for the condensation of SCT-(TCHO)₄ with IC or FIC. This can be attributed to the different acidity of these compounds. For comparison, the corresponding linear A-D-A molecules were also synthesized via similar synthetic approaches. Except CPDT-(TIC)₂, which was reported in our previous paper,²⁷ both CPDT-(TID)₂ and CPDT-(TFIC)₂ were reported here for the first time. All the intermediates and the final compounds were fully characterized by ¹H NMR, ¹³C NMR, and mass spectrometry (see the Supporting Information for more details).

Photophysical and Electrochemical Properties. Figure 1a and 1c depict the absorption and fluorescence spectra of

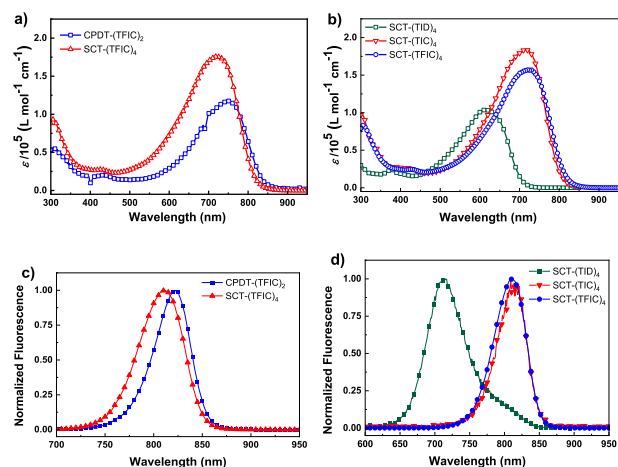


Figure 1. (a) UV-vis absorption and (c) fluorescence spectra of SCT-(TFIC)₄, CPDT-(TFIC)₂ in solution of CHCl₃; (b) UV-vis absorption and (d) fluorescence spectra of SCT-(TFIC)₄, SCT-(TIC)₄, and SCT-(TID)₄ in solution of CHCl₃.

SCT-(TFIC)₄ and CPDT-(TFIC)₂ in chloroform solution. As seen here, both compounds showed the intramolecular charge transfer absorption bands over 500–750 nm. Surprisingly, the spiro-derivative SCT-(TFIC)₄ showed a shorter absorption maximum ($\lambda_{\text{max}} = 725$ nm) and fluorescence maximum wavelengths ($\lambda_{\text{fl}}^{\text{max}} = 810$ nm) than CPDT-(TFIC)₂ (750 and 847 nm, respectively, Table 1). Similar phenomena were also measured for IC and ID terminated compounds (Figure S1), suggesting that there is no π -electron delocalization over the central carbon atom, which is different from the literature reported spiro-fluorene compounds where a spiro-conjugation effect was obviously observed.^{12,27} The detailed reason for the absence of spiro-conjugation in the SCT series is not clear. We speculate that this may be due to the fact that the frontier orbital of the conjugated A-D-A moiety is far away from the central sp³ carbon atom and there is no direct interaction between two branches in the ground state. However, further experiments are still needed to fully understand the detailed mechanism. Interestingly, although there are two identical linear motifs in the spiro molecules, they showed 1.5–1.6 times of $\epsilon_{\text{abs}}^{\text{max}}$ than the corresponding linear ones. This phenomenon was also reported by Dalinot et al. in the SBF based compounds and was ascribed to the limitation of chromophore rotation through the spiro-conjugation structure.^{28,29} The comparison on the absorption spectra of SCT-(TID)₄, SCT-(TIC)₄, and SCT-(TFIC)₄ showed that the IC and FIC terminated compounds have red-shifted absorption bands (Figure 1b), which was ascribed to the stronger electron-withdrawing capability of IC and FIC units. In thin solid film, all these compounds showed red-shifted absorption band (Figure S2), suggesting certain π - π interactions for these compounds in solid state. The optical band gaps for these compounds were estimated from the absorption onset of the solid films, and values of 1.51, 1.55, and 1.75 eV were determined for SCT-(TFIC)₄, SCT-(TIC)₄, and SCT-(TID)₄, respectively. As expected, the stronger electron-withdrawing nature of terminal accepting moiety decreases the bandgap.

Figure 2a and Figure S5 depicts the cyclic voltammograms (CV) of spiro- and linear compounds measured in CH₂Cl₂ solution. For the linear compounds, two reversible oxidation processes were measured, which are ascribed to the oxidation of the central π -conjugation unit to mono- and bications, respectively. Slightly higher first oxidation potential ($E_{\text{ox}}^{\text{01}}$) for the FIC terminated compound (0.53 V) than that of IC (0.47 V) and ID (0.43 V) analogues indicates that the terminal electron accepting unit has certain influence on the oxidation process on

Table 1. Photophysical and Electrochemical Data of SCT and CPDT Derivatives

compound	optical data in solution ^a				optical data in thin film ^b			electrochemical data ^c			energy level ^d		
	$\lambda_{\text{max}}^{\text{sol}}$ [nm]	$\epsilon_{\text{max}}^{\text{sol}}$ [L mol ⁻¹ cm ⁻¹] ^e	$\lambda_{\text{onset}}^{\text{sol}}$ [nm]	$\lambda_{\text{fl}}^{\text{max}}$ [nm]	$\lambda_{\text{max}}^{\text{film}}$ [nm]	$\lambda_{\text{onset}}^{\text{film}}$ [nm]	$E_{\text{g}}^{\text{opt}}$ [eV] ^f	$E_{\text{ox}}^{\text{01}}$ [V]	$E_{\text{ox}}^{\text{02}}$ [V]	$E_{\text{red}}^{\text{01}}$ [V]	E_{HOMO} [eV]	E_{LUMO} [eV]	E_{g}^{CV} [V]
SCT-(TFIC) ₄	725	175 700	817	810	758	899	1.51	0.58	0.72	-0.88	-5.57	-4.18	1.39
SCT-(TIC) ₄	715	187 600	801	804	731	893	1.55	0.50	0.65	-0.98	-5.45	-4.04	1.41
SCT-(TID) ₄	614	137 200	707	704	625	776	1.75	0.34	0.46	-1.22	-5.40	-3.93	1.47
CPDT-(TFIC) ₂	750	117 600	847	822	840	925	1.46	0.53	0.89	-0.95	-5.55	-4.19	1.36
CPDT-(TIC) ₂	733	102 000	827	792	794	893	1.47	0.47	0.87	-1.05	-5.54	-4.08	1.43
CPDT-(TID) ₂	624	80 000	726	714	840	–	1.71	0.43	0.89	-1.41	-5.56	-3.86	1.70

^aIn CHCl₃ solution at a concentration of 3.0×10^{-6} mol L⁻¹. ^bIn film. ^cIn CH₂Cl₂ at a concentration of 1.0×10^{-3} mol L⁻¹, with TBAPF₆ (0.1 M) as the support electrolyte and Fc⁺/Fc as reference. ^dCalculated from cyclic voltammetry results, $E_{\text{HOMO}} = -(E_{\text{ox}}^{\text{onset}} + 5.10)$ (eV), $E_{\text{LUMO}} = -(E_{\text{red}}^{\text{onset}} + 5.10)$ (eV), $E_{\text{g}}^{\text{CV}} = (E_{\text{ox}}^{\text{onset}} - E_{\text{red}}^{\text{onset}})$ (eV). ^eMolar absorptivity in solution was obtained by linear fitting absorbance vs concentration. ^fOptical band gap $E_{\text{g}}^{\text{opt}}$ (eV) = $1240/\lambda_{\text{abs}}^{\text{onset}}$.

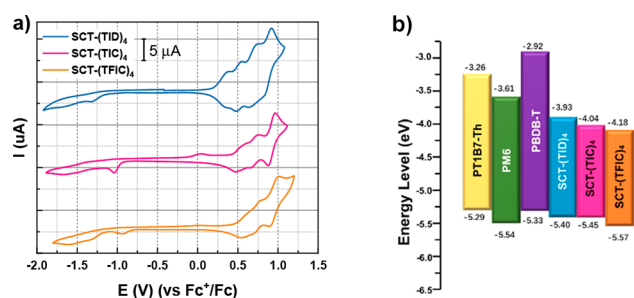


Figure 2. (a) Cyclic voltammograms of SCT derivatives in solution of dichloromethane using TBAPF₆ (0.1 M) as the support electrolyte and at a scan rate of 100 mV s⁻¹. (b) Energy level diagram of donors and acceptors.

the central π -conjugation unit (Table 1). The spiro compounds showed four quasi-reversible oxidation processes over similar potential sweeping range, indicating multiple oxidation processes of the spiro-compounds (see the differential curves of these compounds in Figure S6). The first oxidation potentials ($E_{\text{ox}}^{\text{O1}}$) of SCT-(TFIC)₄, SCT-(TIC)₄ and SCT-(TID)₄ are in the same range to that of the corresponding linear compound (Table 1), indicating that the first oxidation process of spiro-compounds can be ascribed to the oxidation of one of the π -conjugated branches. However, the second oxidation potentials of the spiro-compounds are less than the oxidation of the linear compounds to a bication, showing a different oxidation process for these two series compounds. Knowing that the spiro-compounds has two identical conjugated A-D-A chains, we therefore ascribed the second oxidation process of the SCT compounds to the oxidation of the second π -conjugated branch, yielding a bis(radical-cation), whereas the second oxidation on linear analogue led to dicationic species. Interestingly, oxidation of the second π -conjugated branch is more difficult than the first one. This confirms that because of the linked two π -conjugated systems, the presence of the radical-cation in one π -conjugated system has a significant influence on the oxidation process of the other. Similar as our previous studies,^{30,31} irreversible reduction processes were measured for all these compounds (Figure 2 and Figure S5). The absence of the corresponding oxidation process of the reduced anion indicates that the reduced anions can be easily neutralized in solution. The first reduction potential ($E_{\text{red}}^{\text{O1}}$, Table 1) for the ID terminated SCT-(TID)₄ is measured at -1.22 V, much more negative than corresponding IC and FIC terminated compounds (-0.98 V and -0.88 V, respectively). Similar trends can be observed in the linear analogues. This is ascribed to the weaker electron-withdrawing capacity of the ID groups than IC and FIC groups. These results confirm that the reduction potential is highly related to the terminal electron withdrawing group. In addition, the first reduction potentials ($E_{\text{red}}^{\text{O1}}$, Table 1) for the spiro-compounds SCT-(TFIC)₄, SCT-(TIC)₄ and SCT-(TID)₄ are less negative than corresponding linear analogues CPDT-(TFIC)₂, CPDT-(TIC)₂, and CPDT-

(TID)₂ (-0.88 vs -0.95 V, -0.98 vs -1.05 V, and -1.22 vs -1.41 V, respectively). HOMO/LUMO as well as the energy band gap (E_{g}^{CV}) of these compounds were deduced from the onset oxidation ($E_{\text{ox}}^{\text{onset}}$) and reduction ($E_{\text{red}}^{\text{onset}}$) potentials, and the results are listed in Table 1. All these synthesized molecules showed low-lying LUMO energy level of -3.90 to -4.20 eV, making them suitable for use in polymer solar cells as the electron acceptor in combination with the widely used polymer donor, including PTB7-Th, PBDB-T, and PM6 (Figure 2b). Note that the E_{g}^{CV} is slightly lower than the corresponding $E_{\text{g}}^{\text{opt}}$, which could be ascribed to the different state of the molecules in thin solid films (for UV-vis measurement) and in CH₂Cl₂ solution (for CV measurement).

Photovoltaic Characterizations. The photovoltaic performance for the synthesized materials as the acceptor in polymer solar cells was studied on solar cells adopting an inverted structure (ITO/ZnO/Active layer/MoO₃/Al). Figure 3 shows the current density-voltage (J - V) curves and external

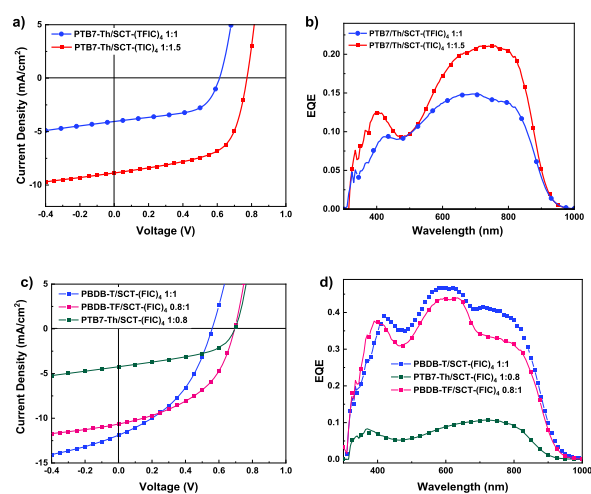


Figure 3. (a) J - V curves and (b) EQE curves of solar cells based on SCT series; (c) J - V curves and (d) EQE curves of solar cells based on SCT-(TFIC)₄ with different donor materials.

quantum efficiency (EQE) plots of optimized devices, and the device performance data are listed in Table 2. For the PTB7-Th based cells, the SCT-(TID)₄ demonstrated very low power conversion efficiency (PCE) of 0.36%, mainly limited by the low short circuit current density ($J_{\text{SC}} = 1.50 \text{ mA/cm}^2$). As for SCT-(TIC)₄ and SCT-(TFIC)₄, the optimized PCE were 2.79% and 2.68%, respectively. Changing the donor from PTB7-Th to PBDB-T and PM6 yields higher J_{SC} of around 12 mA/cm² for these two cells. However, lower V_{OC} and FF limited the overall PCE of 2.90% and 3.73% for the PBDB-T:SCT-(TFIC)₄ and PM6:SCT-(TFIC)₄ cells, respectively. We notice that no obvious correlation between the molecular structure of the acceptor molecules and the photovoltaic performance, which could be due to the different molecular packing of acceptor

Table 2. Device Performance Based on SCT Series

acceptor	donor	ratio (D:A)	V_{OC} (V)	J_{SC} (mA/cm ²)	FF (%)	PCE (%)
SCT-(TID) ₄	PTB7-Th	1:1	0.701	1.21	0.319	0.27
SCT-(TIC) ₄		1:1.5	0.780	6.06	0.591	2.79
SCT-(TFIC) ₄		1:0.8	0.775	5.68	0.609	2.68
SCT-(TFIC) ₄	PBDB-T	1:1	0.559	12.86	0.403	2.90
SCT-(TFIC) ₄	PM6	1:1.25	0.692	11.49	0.470	3.73

molecules within the photoactive layer. However, further optimization of the nanomorphology of the photoactive layer is needed (see AFM topological morphology of the PM6:SCT-(TFIC)₄ in Figure S8). Nevertheless, the current work proved that SCT can be a useful building block for constructing 3D conjugated molecules for use in organic electronics.

CONCLUSION

In this work, we have developed a new synthetic approach to brominated 4,4'-spirobi[cyclopenta[2,1-*b*;3,4-*b'*]dithiophene] core (SCT-Br₄). By using a structurally symmetric 3,3'-dibromo-5,5'-bis(trimethylsilyl)-2,2'-bithiophene as the precursor for the synthesis of two key intermediates, the synthetic route was significantly simplified in comparison to the previous reported method. Functionalization of the spiro core to A-D-A type conjugated molecules were performed with different electron accepting terminal moieties. The optical and electrochemical properties of these A-D-A type molecules can be tuned by changing the terminal electron definition moiety. Except devices fabricated with PTB7-Th:SCT-(TID)₄ blend, all other fabricated polymer solar cells exhibited PCE ranging from 2.5–4%. The current work demonstrates a new family of conjugated 3D molecules for organic electronics.

EXPERIMENTAL SECTION

General Methods. All chemicals and solvents were reagent grade and used as received without further purification unless specified. The dry solvent is collected from PURESULV Solvent Purification systems PS-MD-SON7 (Innovative Technology). N-bromo succinimide was recrystallized according to the published handbook. Heating was conducted on a heating mantle. Reactions were tracked by thin layer chromatography (TLC) that was conducted on an aluminum substrate coated with silica gel Si 60-F254 (Merck, Germany) and by ¹H NMR spectrum. Column chromatography was carried out on silica gel (Sinopharm, China), mesh size 0.075–0.15 mm (normal) or 0.037–0.075 mm (flash). Nuclear magnetic resonance (NMR) such as ¹H NMR and ¹³C NMR was recorded on a Bruker Ascend TM 400 MHz in deuterated chloroform (CDCl₃) using TMS as an internal reference. MALDI-TOF-MS spectra were obtained on Bruker Auto Bending Speed LRF using *trans*-2-[3-(4-*tert*-butylphenyl)-2-methyl-2-propenyl]malononitrile (DCTB) as a matrix substrate. Compounds 1, 2, and 4 were synthesized according to the literature.^{23,24}

Synthesis. **2-Bromo-5-trimethylsilyl-thiophene (1).** To a solution of 2-bromothiophene (29.98 g, 0.18 mol, 1.0 equiv) in dried THF (200 mL) under argon was added LDA (2.0 M in THF/hexane, 101 mL, 0.20 mol, 1.1 equiv) under –78 °C. The mixture was stirred for 1 h under this temperature, forming a dark brown solution. Trimethyl chlorosilane (13.5 mL, 0.18 mol, 1.0 equiv) was carefully added at this temperature, and the resulted mixture was warmed to rt and further stirred overnight. After clear formation of intermediate 2 was confirmed by TLC study, the in situ generated mixture was quenched with water. The solvent was removed, and the residue dissolved in PE then washed with water, dried with Na₂SO₄, and the solvent was removed from vacuum affording red oil. Further distillation under reduced pressure (130 mPa, 120 °C) afforded pure product as colorless oil (61%) ¹H NMR (400 MHz, CDCl₃) δ [ppm] = 7.08 (d, *J* = 3.5 Hz, 1H), 6.99 (d, *J* = 3.5 Hz, 1H), 0.33 (s, 9H).

(3,3'-Dibromo-[2,2'-bithiophene]-5,5'-diyl)bis(trimethylsilane) (2). To a cold solution (–78 °C) of 1 (28.87 g, 123 mmol, 1.0 equiv) in dried THF (190 mL) under nitrogen was carefully added a solution of LDA (2M/hexane/THF, 71 mL, 141 mmol, 1.1 equiv) through a dropping funnel in dropwise manner. The colorless solution gradually turned to coffee brown and partial participation of lithium salt was observed. The suspension was stirred for 1 h under this temperature and the completion of halogen dance reaction was confirmed by ¹H NMR study. Addition of CuCl₂ (18.87 g, 141 mmol) was introduced by one portion afterward, resulting in dark green solution. The mixture was

slowly warmed up to room temperature and was stirred overnight, which was subsequently worked up by quenching with methanol, concentrated, and filtrated on Celite pad to afford dark brown oil. The oil was further purified on column chromatography (hexane) to give pure product as yellow crystals in 20.47 g (74% yield). ¹H NMR (400 MHz, CDCl₃) δ [ppm] = 7.15 (s, 2H), 0.34 (s, 27H). ¹³C{¹H} NMR (100 MHz, CDCl₃) δ [ppm] = 143.1, 137.2, 134.1, 113.1, –0.2

2,6-Bis(trimethylsilyl)-4H-cyclopenta[2,1-*b*:3,4-*b'*]dithiophen-4-one (4). To a solution of 2 (1.10 g, 2.14 mmol, 1.0 equiv) in dried THF (10 mL) under argon was added n-BuLi (2.2 M in hexane, 2.0 mL, 4.28 mmol, 2.0 equiv) at –78 °C. The glass yellow solution was stirred for 25 min under this temperature. A small portion of the mixture was quenched with MeOH and the completion of the lithium–halogen exchange was proved by ¹H NMR. Addition of NMe₂COCl (0.3 mL, 2.56 mmol, 5.0 equiv) was carefully introduced under –78 °C and the resulted mixture turned to light red solution, which was warmed to 0 °C and further stirred for 90 min. The resulted mixture was quenched with saturated NH₄Cl. Formation of blood red mixture with white participate were observed. The solvent was removed, and the residue was extracted with PE, washed with H₂O, and dried with Na₂SO₄. Solvent was removed to afford the crude product as blood-red oil. The oil was purified by chromatography (3% EtOAc/PE) to afford 540 mg pure product as red solid (85% yield). ¹H NMR (400 MHz, CDCl₃) δ [ppm] = 7.07 (s, 2H), 0.31 (s, 18H). ¹³C{¹H} NMR (100 MHz, CDCl₃) δ [ppm] = 183.2, 154.4, 144.9, 144.2, 127.9, 0.2.

4-(5,5'-Bis(trimethylsilyl)-[2,2'-bithiophen]-3-yl)-2,6-bis(trimethylsilyl)-4H-cyclopenta[2,1-*b*:3,4-*b'*]dithiophen-4-ol (5). To a solution of 2 (3.05 g, 6.5 mmol, 1.1 equiv) in dried ether (30 mL) under argon was added dropwise n-BuLi (2.5 M in hexane, 5.2 mL, 13 mmol, 2.2 equiv) at –80 °C. The glass yellow solution was stirred for 25 min under this temperature. Solution of 4 (2.05 g, 6.1 mmol, 1.0 equiv) in dried ether (30 mL) was carefully added to the mixture. The resulted orange suspension was stirred under ice bath for 1 h and the reaction was then quenched with saturated NH₄Cl. The aqueous phase was extracted with DCM (50 mL) for 3 times, and the combined organic phase was washed with water (100 mL), dried with Na₂SO₄ and concentrated under reduced pressure to afford dark red oil (2.97 g), which was purified on chromatography (20% DCM/PE) to afford pure product as brown powders (2.8 g, 71%) ¹H NMR (400 MHz, CDCl₃) δ [ppm] = 7.53 (s, 1H), 6.87 (d, *J* = 4.8 Hz, 3H), 6.47 (d, *J* = 3.4 Hz, 1H), 2.48 (s, 1H), 0.33 (s, 9H), 0.26 (s, 27H) ¹³C{¹H} NMR (100 MHz, CDCl₃) δ [ppm] = 158.4, 142.9, 141.9, 141.6, 139.3, 139.1, 139.0, 136.6, 135.1, 133.4, 129.2, 128.6, –0.2 MS (MALDI–TOF) calcd. for C₂₉H₄₂OS₄Si₄ *m/z* = 644.86 [M]⁺, found 644.74.

2,6-Dibromo-4-(5,5'-dibromo-[2,2'-bithiophen]-3-yl)-4H-cyclopenta[2,1-*b*:3,4-*b'*]dithiophen-4-ol (6). To a solution of 4 (1.03 g, 1.53 mmol, 1.0 equiv) in dried chloroform (15 mL) under nitrogen was added NBS (1.15 g, 6.46 mmol, 4.2 equiv) at –25 °C. The dark brown solution was stirred for 1.5 h under this temperature. The resulted mixture was washed with water, extracted with chloroform (3 × 10 mL), dried and concentrated to afford brown oil (1.3 g), which was purified by column chromatography (DCM/PE to 20% Acetone/PE) to afford pure product as brown powders. (79%) ¹H NMR (400 MHz, CDCl₃) δ [ppm] = 7.35 (s, 1H), 6.84 (s, 2H), 6.76 (d, *J* = 4 Hz, 1H), 6.24 (d, *J* = 4 Hz, 1H), 2.38 (s, 1H) ¹³C{¹H} NMR (100 MHz, CDCl₃) δ [ppm] = 153.2, 138.1, 137.1, 133.3, 130.7, 130.5, 129.3, 129.2, 124.9, 114.4, 112.9, 112.3, 77.7. MS (MALDI–TOF) calcd. for C₁₇H₆Br₄OS₄ *m/z* = 672.5 [M]⁺, found 672.11.

2,2',6,6'-Tetrabromo-4,4'-spirobi[cyclopenta[2,1-*b*:3,4-*b'*]dithiophene] SCT-Br₄. To a solution of BF₃·OEt₂ (1 mL, 7.5 mmol, 5.0 equiv) in dried DCM (700 mL) under argon was added dropwise a solution of 6 (0.997 g, 1.5 mmol, 1.0 equiv) in dried DCM (60 mL). The colorless solution turned dark green for 30 min, and the TLC indicated completion of the reaction. The dark green solution was concentrated, washed with water (100 mL), and dried with Na₂SO₄. The solvent was removed to afford green powders (1.5 g), which was purified by column chromatography (PE to 50% DCM in PE) to afford product SCT-Br₄ as brown powders (69%). ¹H NMR (400 MHz, CDCl₃) δ [ppm] = 6.54 (s, 4H). ¹³C{¹H} NMR (100 MHz, CDCl₃) δ

[ppm] = 146.7, 138.6, 123.9, 112.3, 58.3. MS (MALDI–TOF) calcd. for m/z = $C_{17}H_{14}S_4Br_4$ 655.59 $[M]^+$, found 655.36.

5,5',5'',5'''-(4,4'-Spirobicyclopenta[2,1-b:3,4-b']dithiophene)-2,2',6,6'-tetrayl)tetrakis(4-hexylthiophene-2-carbaldehyde) SCT-(TCHO)₄. A mixture of SCT-Br₄ (500 mg, 0.76 mmol, 1.0 equiv) with B-Tc₆-CHO (6.0 equiv), Pd₂(dba)₃ (77 mg, 0.076 mmol, 0.1 equiv), PH(*t*-Bu₃)BF₄ (45 mg, 0.15 mmol, 0.2 equiv) was taken in a predried, 100 mL, two-necked, round-bottomed flask fitted with a condenser, a magnetic stir bar and an argon inlet. THF (50 mL) was added followed by K₂CO₃ solution (1M, 10 mL, 8.0 equiv). The dark red mixture was refluxed under argon for 16 h (on a heating mantle), which was further extracted with DCM (20 mL) for 3 times, washed with water (250 × 3 mL), dried with Na₂SO₄, and concentrated under reduced pressure to afford dark orange oil. The oil was purified by column chromatography eluting with 50% DCM in hexane and gel permeation chromatography (GPC) eluting with THF to afford product as orange-red solid (60%). ¹H NMR (400 MHz, CDCl₃) δ [ppm] = 9.78 (s, 4H), 7.55 (s, 4H), 6.81 (s, 4H), 2.81 (t, *J* = 12 Hz, 8H), 1.36 (m, 32H), 0.85 (t, *J* = 12 Hz, 12H). ¹³C{¹H} NMR (100 MHz, CDCl₃) δ [ppm] = 182.4, 150.4, 141.1, 140.5, 140.3, 138.9, 137.3, 121.2, 31.6, 30.1, 29.6, 29.1, 22.6, 14.1. MS (MALDI–TOF) calcd. for C₆₁H₆₄O₄S₈ m/z = 1116.26 $[M]^+$, found 1116.91.

2,2',2'',2'''-((4,4'-Spirobicyclopenta[2,1-b:3,4-b']dithiophene)-2,2',6,6'-tetrayl)tetrakis(4-hexylthiophene-5,2-diyl)tetrakis(methaneylylidene)tetrakis(1H-indene-1,3(2H)-dione) SCT-(TID)₄. SCT-(TCHO)₄ (400 mg, 358 μmol), and 1H-indene-1,3(2H)-dione (ID) (310 mg, 2.15 mmol) was dissolved in 120 mL CHCl₃. The reaction was heated to 65 °C (on a heating mantle). 0.1 mL piperidine was added dropwise as the base for this reaction. The reaction was monitored by TLC and mass (MALDI–TOF). After stirring 18 h, the reaction mixture was concentrated and was recrystallized in MeOH, 650 mg dark blue solid was obtained as crude product. The crude product was purified by column chromatography on silica gel eluting with 5% DCM/PE to give preliminary product. The product was further purified by gel permeation chromatography eluting with THF to afford pure product as dark blue solids. (410 mg, 70%) ¹H NMR (400 MHz, CDCl₃) δ [ppm] = 8.03–7.46 (broad, 24H), 3.03–2.65 (broad, 8H), 1.28–1.19 (broad, 32H), 1.03–0.79 (broad, 12H); ¹³C{¹H} NMR (100 MHz, CDCl₃) δ [ppm] = 141.9, 134.8, 122.6, 21.8, 29.9, 29.7, 29.6, 22.8, 14.2; MS (MALDI–TOF) calcd. for C₉₇H₈₀O₈S₈ m/z = 1628.36 $[M]^+$, found 1628.39.

2,2',2'',2'''-((2E,2'E,2''E,2'''E)-((4,4'-Spirobicyclopenta[2,1-b:3,4-b']dithiophene)-2,2',6,6'-tetrayl)tetrakis(4-hexylthiophene-5,2-diyl)tetrakis(methaneylylidene)tetrakis(3-oxo-2,3-dihydro-1H-indene-2,1-diyldene)tetramalononitrile) SCT-(TIC)₄. SCT-(TCHO)₄ (400 mg, 358 μmol), and 2-(3-oxo-2,3-dihydro-1H-inden-1-ylidene)-malononitrile (IC) (420 mg, 2.15 mmol) was dissolved in 120 mL CHCl₃. The reaction was heated to 65 °C (on a heating mantle). 0.1 mL pyridine was added dropwise as the base for this reaction. The reaction was monitored by TLC and mass (MALDI–TOF). After stirring 18 h, the reaction mixture was concentrated and was recrystallized in MeOH, 700 mg dark blue solid was obtained as crude product. The crude product was purified by column chromatography on silica gel eluting with 5% DCM/PE to give preliminary product. The product was further purified by gel permeation chromatography eluting with THF to afford pure product as dark blue solids. (540 mg, 85%) ¹H NMR (400 MHz, CDCl₃) δ [ppm] = 7.99–7.50 (broad, 24H), 3.03–2.65 (broad, 8H), 1.89–1.03 (broad, 32H), 1.02–0.71 (broad, 12H); ¹³C{¹H} NMR (100 MHz, CDCl₃) δ [ppm] = 159.8, 148.8, 142.0, 140.3, 139.4, 136.6, 135.0, 133.7, 123.5, 122.1, 114.6, 114.1, 31.7, 30.3, 30.0, 29.7, 22.7, 14.2; MS (MALDI–TOF) calcd. for C₁₀₉H₈₀N₈O₄S₈ m/z = 1821.41 $[M]^+$, found 1820.91.

2,2',2'',2'''-((2E,2'E,2''E,2'''E)-((4,4'-Spirobicyclopenta[2,1-b:3,4-b']dithiophene)-2,2',6,6'-tetrayl)tetrakis(4-hexylthiophene-5,2-diyl)tetrakis(methaneylylidene)tetrakis(5,6-difluoro-3-oxo-2,3-dihydro-1H-indene-2,1-diyldene)tetramalononitrile) SCT-(TFIC)₄. A mixture of SCT-(TCHO)₄ (230 mg, 0.21 mmol, 1.0 equiv) and 5,6-difluoro-1H-indene-1,3(2H)-dione (FIC) (284 mg, 1.23 mmol, 6.0 equiv) was dissolved in chloroform and was heated to 50 °C (on a heating mantle). Pyridine (0.5 mL) was then added. The dark blue solution was further refluxed for 18 h and was concentrated and purified

by column chromatography eluting with 50% DCM in hexane. The resulted residue was recrystallized with methanol to give the target product as dark blue solid. (240 mg, 60%). ¹H NMR (400 MHz, CDCl₃) δ [ppm] = 8.66–6.67 (broad, 20H), 3.10–2.76 (broad, 8H), 0.88–2.03 (broad, 44H); ¹³C{¹H} NMR (100 MHz, CDCl₃) δ [ppm] = 157.6, 148.5, 140.8, 136.6, 135.7, 133.6, 114.5, 112.9, 31.7, 30.2, 39.7, 24.7, 22.8, 14.2; MS (MALDI–TOF) calcd. for C₁₀₉H₇₂F₈N₈O₄S₈ m/z = 1964.33 $[M]^+$, found 1964.91.

5,5'-(4,4-Bis(2-ethylhexyl)-4H-cyclopenta[2,1-b:3,4-b']dithiophene-2,6-diyl)bis(4-hexylthiophene-2-carbaldehyde) CPDT-(TCHO)₂. A mixture of CPDT-Br₂ (500 mg, 0.89 mmol, 1.0 equiv) mixing with B-Tc₆-CHO (862 mg, 2.67 mmol, 3.0 equiv), Pd₂(dba)₃ (82 mg, 0.089 mmol, 0.1 equiv), PH(*t*-Bu₃)BF₄ (51 mg, 0.18 mmol, 0.2 equiv), was taken in a predried, 100 mL, two-necked, round-bottomed flask fitted with a condenser, a magnetic stir bar and an argon inlet. THF (50 mL) was added followed by K₂CO₃ solution (1M, 4 mL, 8.0 equiv). The dark red mixture was refluxed under argon for 16 h, which was further extracted with DCM (20 mL) for 3 times, washed with water (250 × 3 mL), dried with Na₂SO₄, and concentrated under reduced pressure to afford dark orange oil. The oil was purified by column chromatography eluting with 50% DCM in hexane to give pure product as red-orange oil (585 mg, 83%). ¹H NMR (400 MHz, CDCl₃) δ [ppm] = 9.83 (s, 2H), 7.60 (s, 2H), 7.17–7.15 (t, *J* = 8 Hz, 2H), 2.85–2.82 (t, *J* = 6 Hz, 4H), 1.97–1.89 (m, 4H), 1.72–1.69 (m, 4H), 1.43–1.24 (m, 28H), 1.01–0.91 (m, 28H), 0.73–0.62 (m, 16H); ¹³C{¹H} NMR (100 MHz, CDCl₃) δ [ppm] = 182.4, 158.6, 142.1, 139.9, 139.1, 138.77, 135.4, 122.6, 54.3, 43.1, 35.2, 34.3, 31.6, 30.2, 29.7, 29.5, 29.2, 28.6, 27.4, 22.7, 22.6, 14.1, 10.7; MS (MALDI–TOF) calcd. for C₄₇H₆₆O₂S₄ m/z = 790.39 $[M]^+$, found 790.13.

2,2'-(((4,4-Bis(2-ethylhexyl)-4H-cyclopenta[2,1-b:3,4-b']dithiophene-2,6-diyl)bis(4-hexylthiophene-5,2-diyl))bis(methaneylylidene))bis(1H-indene-1,3(2H)-dione) CPDT-(TID)₂. CPDT-(TCHO)₂ (200 mg, 252 μmol), and 1H-indene-1,3(2H)-dione (ID) (55 mg, 756 μmol) was dissolved in 20 mL CHCl₃. The reaction was heated to 65 °C (on a heating mantle). 0.1 mL pyridine was added dropwise as the base for this reaction. The reaction was monitored by TLC and mass (MALDI–TOF). After stirring 18 h, the reaction mixture was concentrated and was recrystallized in MeOH, 210 mg dark blue solid was obtained as crude product. The crude product was purified by column chromatography on silica gel eluting with 25% DCM/PE to give preliminary product. The product was further recrystallized in MeOH to afford pure product as dark blue solids. (185 mg, 71%) ¹H NMR (400 MHz, CDCl₃) δ [ppm] = 7.99 (t, *J* = 8 Hz, 8H), 7.92 (s, 4H), 7.87–7.75 (m, 12H), 7.44 (t, *J* = 8 Hz, 4H), 2.91 (t, *J* = 8 Hz, 8H), 2.03 (m, 8H), 1.79 (m, 8H), 1.50–1.25 (m, 24H), 1.11–0.71 (m, 44H), 0.71–0.65 (m, 24H); ¹³C{¹H} NMR (100 MHz, CDCl₃) δ [ppm] = 190.2, 189.9, 159.5, 146.4, 145.8, 142.0, 140.4, 139.7, 136.5, 135.6, 134.9, 134.7, 134.3, 123.5, 122.9, 122.8, 122.7, 54.3, 43.2, 35.4, 34.2, 31.7, 30.0, 29.7, 29.6, 28.6, 27.4, 22.8, 22.6, 14.1, 14.05, 10.7; MS (MALDI–TOF) calcd. for C₆₅H₇₄O₄S₄ m/z = 1047.54 $[M]^+$, found 1047.22.

2,2'-((2E,2'E)-(((4,4-Bis(2-ethylhexyl)-4H-cyclopenta[2,1-b:3,4-b']dithiophene-2,6-diyl)bis(4-hexylthiophene-5,2-diyl))bis(methaneylylidene))bis(3-oxo-2,3-dihydro-1H-indene-2,1-diyldene))dimalononitrile) CPDT-(TIC)₂. A mixture of CPDT-(TCHO)₂ (300 mg, 0.37 mmol, 1.0 equiv) and 3-(dicyanomethylidene)indan-1-one (220 mg, 1.13 mmol, 3.0 equiv) was dissolved in chloroform and was heated to 50 °C (on a heating mantle). Pyridine (0.5 mL) was then added. The dark blue solution was further refluxed for 18 h and was concentrated and purified by column chromatography eluting with 50% DCM in hexane. The resulted residue was recrystallized with methanol to give pure product as dark blue solid (450 mg, 64%). ¹H NMR (400 MHz, CDCl₃) δ [ppm] = 8.80 (s, 2H), 8.71–8.69 (d, *J* = 8 Hz, 2H), 7.95–7.93 (d, *J* = 8 Hz, 2H), 7.78–7.74 (t, *J* = 8 Hz, 4H), 7.67 (s, 2H), 7.50–7.47 (t, *J* = 6 Hz, 2H), 2.81–2.87 (t, *J* = 8 Hz, 4H), 2.03–2.00 (m, 4H), 1.79–1.75 (m, 8H), 1.47–1.38 (m, 12H), 1.03–0.93 (m, 20H), 0.73–0.67 (m, 14H); ¹³C{¹H} NMR (100 MHz, CDCl₃) δ [ppm] = 189.3, 160.9, 158.8, 149.8, 147.4, 142.9, 140.1, 137.1, 136.9, 135.1, 133.6, 126.0, 123.7, 123.3, 122.1, 113.72, 69.0, 54.1, 43.4, 35.4, 34.2, 32.1, 29.9, 29.6, 29.4,

28.6, 27.4, 22.8, 22.6, 14.1, 10.7; MS (MALDI-TOF) calcd. for $C_{71}H_{74}N_4O_2S_4$ $m/z = 1142.47$ [M]⁺, found 1142.26.

2,2'-((2E,2'E)-((4,4-Bis(2-ethylhexyl)-4H-cyclopenta[2,1-b:3,4-b']dithiophene-2,6-diyl)bis(4-hexylthiophene-5,2-diyl))bis(methanelylidene))bis(5,6-difluoro-3-oxo-2,3-dihydro-1H-indene-2,1-diylidene)dimalononitrile CPDT-(TFIC)₂. A mixture of CPDT-(TCHO)₂ (320 mg, 0.51 mmol, 1.0 equiv) and 2-(5,6-Difluoro-3-oxo-2,3-dihydro-1H-inden-1-ylidene)malononitrile (360 mg, 1.54 mmol, 3.0 equiv) was dissolved in chloroform and was heated to 50 °C (on a heating mantle). Pyridine (0.5 mL) was then added. The dark blue solution was further refluxed for 18 h and was concentrated and purified by column chromatography eluting with 50% DCM in hexane. The resulted residue was recrystallized with methanol to give pure product as dark blue solid (324 mg, 70%). ¹H NMR (400 MHz, CDCl₃) δ [ppm] = 8.76 (s, 2H), 8.54–8.51 (t, J = 6 Hz, 2H), 7.70–7.67 (m, 4H), 7.50–7.48 (t, J = 4 Hz, 2H), 2.90–2.87 (t, J = 6 Hz, 4H), 2.04–1.98 (m, 4H), 1.78–1.74 (m, 4H), 1.48–1.38 (m, 14H), 1.04–0.92 (m, 28H), 0.74–0.66 (m, 16H); ¹³C{¹H} NMR (100 MHz, CDCl₃) δ [ppm] = 186.1, 160.6, 158.2, 155.4, 153.4, 150.7, 148.9, 141.2, 137.2, 136.6, 134.4, 134.1, 123.5, 122.1, 115.0, 114.2, 112.5, 69.5, 54.5, 43.3, 35.4, 34.1, 31.6, 29.8, 29.7, 29.3, 28.6, 27.4, 22.8, 14.1, 10; MS (MALDI-TOF) calcd. for $C_{71}H_{70}F_4N_4O_2S_4$ $m/z = 1214.43$ [M]⁺, found 1214.60.

ASSOCIATED CONTENT

Supporting Information

The Supporting Information is available free of charge at <https://pubs.acs.org/doi/10.1021/acs.joc.1c02848>.

Additional experimental details, materials, methods, characterization data (UV-vis, fluorescence, ¹H, ¹³C, and mass spectra, cyclic voltammograms), and solar cell performance data (PDF)

AUTHOR INFORMATION

Corresponding Author

Yi Lin – Department of Chemistry, Xi'an Jiaotong-Liverpool University, Suzhou 215000, PR China; orcid.org/0000-0001-9478-152X; Email: Yi.Lin@xjtlu.edu.cn

Authors

Xiao Chen Liu – Department of Chemistry, Xi'an Jiaotong-Liverpool University, Suzhou 215000, PR China
 Yuanxun Zhang – Department of Chemistry, Xi'an Jiaotong-Liverpool University, Suzhou 215000, PR China
 Jianchang Wu – i-Lab & Printable Electronics Research Center, Suzhou Institute of Nano-Tech and Nano-Bionics, Chinese Academy of Sciences, Suzhou 215123, PR China
 Yuchao Ma – i-Lab & Printable Electronics Research Center, Suzhou Institute of Nano-Tech and Nano-Bionics, Chinese Academy of Sciences, Suzhou 215123, PR China
 Kim K. T. Lau – Department of Chemistry, Xi'an Jiaotong-Liverpool University, Suzhou 215000, PR China
 Jin Fang – i-Lab & Printable Electronics Research Center, Suzhou Institute of Nano-Tech and Nano-Bionics, Chinese Academy of Sciences, Suzhou 215123, PR China
 Chang-Qi Ma – i-Lab & Printable Electronics Research Center, Suzhou Institute of Nano-Tech and Nano-Bionics, Chinese Academy of Sciences, Suzhou 215123, PR China; orcid.org/0000-0002-9293-5027

Complete contact information is available at: <https://pubs.acs.org/doi/10.1021/acs.joc.1c02848>

Notes

The authors declare no competing financial interest.

ACKNOWLEDGMENTS

This work has obtained financial support from Xi'an Jiaotong-Liverpool University Research Development Fund (RDF-14-02-46) and Xi'an Jiaotong-Liverpool University Key Program Special Fund (KSF-E-55).

REFERENCES

- Wang, S.; Zhang, H.; Zhang, B.; Xie, Z.; Wong, W.-Y. Towards high-power-efficiency solution-processed OLEDs: Material and device perspectives. *Materials Science and Engineering: R: Reports* **2020**, *140*, 100547.
- Liu, Q.; Bottle, S. E.; Sonar, P. Developments of Diketopyrrolopyrrole-Dye-Based Organic Semiconductors for a Wide Range of Applications in Electronics. *Adv. Mater.* **2020**, *32* (4), 1903882.
- Liang, S.; Jiang, X.; Xiao, C.; Li, C.; Chen, Q.; Li, W. Double-Cable Conjugated Polymers with Pendant Rylene Diimides for Single-Component Organic Solar Cells. *Acc. Chem. Res.* **2021**, *54* (9), 2227–2237.
- Kini, G. P.; Jeon, S. J.; Moon, D. K. Latest Progress on Photoabsorbent Materials for Multifunctional Semitransparent Organic Solar Cells. *Adv. Funct. Mater.* **2021**, *31* (15), 2007931.
- Gangala, S.; Misra, R. Spiro-linked organic small molecules as hole-transport materials for perovskite solar cells. *J. Mater. Chem. A* **2018**, *6* (39), 18750–18765.
- Jia, L.; Chen, M.; Yang, S. Functionalization of fullerene materials toward applications in perovskite solar cells. *Mater. Chem. Front.* **2020**, *4* (8), 2256–2282.
- Zhang, Z.-G.; Li, Y. Polymerized Small-Molecule Acceptors for High-Performance All-Polymer Solar Cells. *Angew. Chem., Int. Ed.* **2021**, *60* (9), 4422–4433.
- Lin, Y.; Zhan, X. Oligomer Molecules for Efficient Organic Photovoltaics. *Acc. Chem. Res.* **2016**, *49* (2), 175–183.
- Liang, N.; Meng, D.; Wang, Z. Giant Rylene Imide-Based Electron Acceptors for Organic Photovoltaics. *Acc. Chem. Res.* **2021**, *54* (4), 961–975.
- Saeed, M. A.; Le, H. T. M.; Miljanić, O. Š. Benzobisoxazole Cruciforms as Fluorescent Sensors. *Acc. Chem. Res.* **2014**, *47* (7), 2074–2083.
- Ma, C.-Q. Conjugated dendritic oligothiophenes for solution-processed bulk heterojunction solar cells. *Frontiers of Optoelectronics in China* **2011**, *4* (1), 12.
- Liu, S.; Xia, D.; Baumgarten, M. Rigidly Fused Spiro-Conjugated π -Systems. *ChemPlusChem* **2021**, *86* (1), 36–48.
- Wu, X.-F.; Fu, W.-F.; Xu, Z.; Shi, M.; Liu, F.; Chen, H.-Z.; Wan, J.-H.; Russell, T. P. Spiro Linkage as an Alternative Strategy for Promising Nonfullerene Acceptors in Organic Solar Cells. *Adv. Funct. Mater.* **2015**, *25* (37), 5954–5966.
- Chang, M.; Wang, Y.; Qiu, N.; Yi, Y.-Q.; Wan, X.; Li, C.; Chen, Y. A Three-dimensional Non-fullerene Small Molecule Acceptor for Solution-processed Organic Solar Cells. *Chin. J. Chem.* **2017**, *35* (11), 1687–1692.
- Gao, G.; Liang, N.; Geng, H.; Jiang, W.; Fu, H.; Feng, J.; Hou, J.; Feng, X.; Wang, Z. Spiro-Fused Perylene Diimide Arrays. *J. Am. Chem. Soc.* **2017**, *139* (44), 15914–15920.
- Meng, D.; Wang, R.; Lin, J. B.; Yang, J. L.; Nuryyeva, S.; Lin, Y.-C.; Yuan, S.; Wang, Z.-K.; Zhang, E.; Xiao, C.; Zhu, D.; Jiang, L.; Zhao, Y.; Li, Z.; Zhu, C.; Houk, K. N.; Yang, Y. Chlorinated Spiroconjugated Fused Extended Aromatics for Multifunctional Organic Electronics. *Adv. Mater.* **2021**, *33* (12), 2006120.
- Mishra, A.; Ma, C.-Q.; Bäuerle, P. Functional Oligothiophenes: Molecular Design for Multidimensional Nanoarchitectures and Their Applications. *Chem. Rev.* **2009**, *109* (3), 1141–1276.
- Londenberg, J.; Saragi, T. P. I.; Suske, I.; Salbeck, J. 4,4'-Spiro[*cyclopenta*[2,1-b:3,4-b']dithiophene: A New Generation of Heterocyclic Spiro-Type Molecules. *Adv. Mater.* **2007**, *19* (22), 4049–4053.
- Ohshita, J.; Kondo, K.; Adachi, Y.; Song, M.; Jin, S.-H. Synthesis of spirodithienogermole with triphenylamine units as a dopant-free

hole-transporting material for perovskite solar cells. *J. Mater. Chem. C* **2021**, *9* (6), 2001–2007.

(20) Pan, J.; Wang, L.; Chen, W.; Sang, S.; Sun, H.; Wu, B.; Hang, X.-C.; Sun, Z.; Huang, W. Non-fullerene small molecule acceptors with three-dimensional thiophene/selenophene-annulated perylene diimides for efficient organic solar cells. *J. Mater. Chem. C* **2020**, *8* (20), 6749–6755.

(21) Junyan, D.; Changqi, M.; Yuchao, M.; Hongyu, W.; Jinduo, Y.; Jiabin, Z. Synthesis and Properties of 4,4'-Spiro-bi[cyclopenta[2,1-b;3,4-b']dithiophene]Cored 1,8-Naphthalimide Derivatives for Organic Solar Cells. *Imaging Sci. Photochem.* **2017**, *35* (5), 736–748.

(22) Sun, P.; Sun, H.; Li, X.; Wang, Y.; Shan, H.; Xu, J.; Zhang, C.; Xu, Z.; Chen, Z.-K.; Huang, W. Three dimensional multi-arm acceptors based on diketopyrrolopyrrole with (hetero)aromatic cores for non-fullerene organic solar cells without additional treatment. *Dyes Pigm.* **2017**, *139*, 412–419.

(23) Pozzi, G.; Orlandi, S.; Cavazzini, M.; Minudri, D.; Macor, L.; Otero, L.; Fungo, F. Synthesis and photovoltaic applications of a 4,4'-spirobi[cyclopenta[2,1-b;3,4-b']dithiophene]-bridged donor/acceptor dye. *Org. Lett.* **2013**, *15* (18), 4642–4645.

(24) Getmanenko, Y. A.; Tongwa, P.; Timofeeva, T. V.; Marder, S. R. Base-Catalyzed Halogen Dance Reaction and Oxidative Coupling Sequence as a Convenient Method for the Preparation of Dihalo-bisheteroarenes. *Org. Lett.* **2010**, *12* (9), 2136–2139.

(25) Mari, D.; Miyagawa, N.; Okano, K.; Mori, A. Regiocontrolled Halogen Dance of Bromothiophenes and Bromofurans. *J. Org. Chem.* **2018**, *83* (22), 14126–14137.

(26) Ma, C.-Q.; Mena-Osteritz, E.; Wunderlin, M.; Schulz, G.; Bäuerle, P. 2,2':3',2''-Terthiophene-Based all-Thiophene Dendrons and Dendrimers: Synthesis, Structural Characterization, and Properties. *Chem. - Eur. J.* **2012**, *18* (40), 12880–12901.

(27) Zhang, Y.; Liu, X.; Gu, H.; Yan, L.; Tan, H.; Ma, C.-Q.; Lin, Y. Cyclopentadithiophene cored A- π -D- π -A non-fullerene electron acceptor in ternary polymer solar cells to extend the light absorption up to 900 nm. *Org. Electron.* **2020**, *77*, 105530.

(28) Dalinot, C.; Szalóki, G.; Dindault, C.; Segut, O.; Sanguinet, L.; Leriche, P. Spirobifluorene based small push-pull molecules for organic photovoltaic applications. *Dyes Pigm.* **2017**, *140*, 62–69.

(29) Chiang, C.-L.; Tseng, S.-M.; Chen, C.-T.; Hsu, C.-P.; Shu, C.-F. Influence of Molecular Dipoles on the Photoluminescence and Electroluminescence of Dipolar Spirobifluorenes. *Adv. Funct. Mater.* **2008**, *18* (2), 248–257.

(30) Wang, L.; Zhang, Y.; Yin, N.; Lin, Y.; Gao, W.; Luo, Q.; Tan, H.; Yang, H.-B.; Ma, C.-Q. Correlation of the π -conjugation chain length and the property and photovoltaic performance of benzo[1,2-b:4,5-b']dithiophene-cored A- π -D- π -A type molecules. *Sol. Energy Mater. Sol. Cells* **2016**, *157*, 831–843.

(31) Yin, N.; Wang, L.; Ma, Y.; Lin, Y.; Wu, J.; Luo, Q.; Yang, H.-B.; Ma, C.-Q.; Zhao, X. 4,8-Bis(thienyl)-benzo[1,2-b:4,5-b']dithiophene based A- π -D- π -A typed conjugated small molecules with monothiophene as the π -bridge: Synthesis, properties and photovoltaic performance. *Dyes Pigm.* **2015**, *120*, 299–306.

Recommended by ACS

Design and Synthesis of Annulated Benzothiadiazoles via Dithiolate Formation for Ambipolar Organic Semiconductors

Matthew A. Kolaczowski, Yi Liu, *et al.*

NOVEMBER 10, 2020
ACS APPLIED MATERIALS & INTERFACES

READ 

Tuning of a A-A-D-A-A-Type Small Molecule with Benzodithiophene as a Central Core with Efficient Photovoltaic Properties for Organic Solar Cells

Urwah Azeem, Javed Iqbal, *et al.*

OCTOBER 20, 2021
ACS OMEGA

READ 

Cardanol- and Guaiacol-Sourced Solution-Processable Green Small Molecule-Based Organic Solar Cells

Barla Rajkumar, Bimlesh Lochab, *et al.*

MARCH 30, 2020
ACS SUSTAINABLE CHEMISTRY & ENGINEERING

READ 

Microwave-Assisted Synthesis of Non-Fullerene Acceptors and Their Photovoltaic Studies for High-Performance Organic Solar Cells

Sanchari Shome, Hyosung Choi, *et al.*

AUGUST 18, 2021
ACS APPLIED ENERGY MATERIALS

READ 

Get More Suggestions >